

# Fast Quantum Modular Exponentiation

Rodney Van Meter\* and Kohei M. Itoh†

Graduate School of Science and Technology, Keio University and CREST-JST  
3-14-1 Hiyoshi, Kohoku-ku, Yokohama-shi, Kanagawa 223-8522, Japan

(Dated: July 28, 2004)

We present a detailed analysis of the impact on modular exponentiation of architectural features and possible concurrent gate execution. Various arithmetic algorithms are evaluated for execution time, potential concurrency, and space tradeoffs. We find that, to exponentiate an  $n$ -bit number, for storage space  $100n$  (twenty times the minimum  $5n$ ), we can execute modular exponentiation one hundred to seven hundred times faster than optimized versions of the basic algorithms, depending on architecture, for  $n = 128$ . Addition on a neighbor-only architecture is limited to  $O(n)$  when non-neighbor architectures can reach  $O(\log n)$ , demonstrating that physical characteristics of a computing device have an important impact on both real-world running time and asymptotic behavior. Our results will help guide experimental implementations of quantum algorithms and devices.

PACS numbers: 03.67.Lx, 07.05.Bx, 89.20.Ff

## I. INTRODUCTION

Fundamentally, quantum modular exponentiation, the most computationally intensive part of Shor's factoring algorithm, is  $O(n^3)$  [1, 2, 3]. It consists of  $2n$  modular multiplications, each of which consists of  $O(n)$  additions, each of which requires  $O(n)$  operations. However,  $O(n^3)$  operations do not necessarily require  $O(n^3)$  time steps. On an abstract machine, it is relatively straightforward to see how to reduce each of those three layers to  $O(\log n)$  time steps, in exchange for more space and more *total* gates, giving a total running time of  $O(\log^3 n)$  if  $O(n^3)$  qubits are available and an arbitrary number of gates can be executed concurrently on separate qubits. Such large numbers of qubits are not expected to be practical for the foreseeable future, so much interesting engineering lies in optimizing for a given set of constraints. This paper quantitatively explores those tradeoffs.

This paper is intended to help guide the design and experimental implementation of actual quantum computing devices as the number of qubits grows over the next several generations of devices. Depending on the post-quantum error correction, application-level effective clock rate for a specific technology, choice of exponentiation algorithm may be the difference between hours of computation time and weeks, or between seconds and hours. This difference, in turn, feeds back into the system requirements for the necessary strength of error correction and coherence time.

The Schönhage-Strassen multiplication algorithm is often quoted in quantum computing research as being  $O(n \log n \log \log n)$  for a single multiplication. However, simply citing Schönhage-Strassen without further qualification is misleading for several reasons. Most importantly, the constant factors matter [31]: quantum modular exponentiation based on Schönhage-Strassen is only faster than basic  $O(n^3)$  algorithms for more than approximately 32 kilobits [32]. In

this paper, we will concentrate on smaller problem sizes, and exact, rather than  $O()$ , performance.

Concurrent quantum computation, or circuit depth, is explicitly considered in Cleve and Watrous' parallel implementation of the quantum Fourier transform [4], Gossett's quantum carry-save arithmetic [5], and Zalka's Schönhage-Strassen-based implementation [6]. Moore and Nilsson define the computational complexity class **QNC** to describe certain parallelizable circuits, and show which gates can be performed concurrently, proving that any circuit composed exclusively of CNOTs can be parallelized to be of depth  $O(\log n)$  using  $O(n^2)$  ancillae on an abstract machine [7].

We analyze three separate architectures, still abstract but with some important features that help us understand performance. For all three architectures, we assume any qubit can be the control or target for only one gate at a time. The first, the *AC* architecture, is our abstract model. It supports CCNOT, arbitrary concurrency, and gate operands any distance apart without penalty. It does not support arbitrary control strings on control operations, only CCNOT with two ones as control. The second, the *TC* architecture, is similar but does not support CCNOT, only two-qubit gates. The third architecture, *NTC*, assumes the qubits are laid out in a one-dimensional line, and only neighboring qubits can interact. The 1D layout will have the highest communications costs. Most real, scalable architectures will have constraints with this flavor, if different details, so *TC* and *NTC* can be viewed as bounds within which many real architectures will fall. The layout of variables on this structure has a large impact on performance; what is presented here is the best we have discovered to date, but we do not claim it is optimal.

*NTC* is a reasonable description of several important experimental approaches, including a one-dimensional chain of quantum dots [8], the original Kane proposal [9], and the all-silicon NMR device [10]. Superconducting qubits [11, 12] may map to *TC*, depending on the details of the qubit interconnect.

The difference between *TC* and *NTC* is critical; beyond the important constant factors as nearby qubits shuffle, we will see in section III C that *TC* can achieve  $O(\log n)$  performance

\*Electronic address: rdv@tera.ics.keio.ac.jp

†Electronic address: kitoh@appi.keio.ac.jp

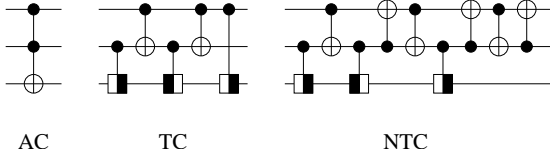


FIG. 1: CCNOT constructions for our three architectures *AC*, *TC*, and *NTC*. The box with the bar on the right represents the square root of  $X$ , and the box with the bar on the left its adjoint.

where  $NTC$  is limited to  $O(n)$ .

For the *TC* and *NTC* architectures, which do not support CCNOT directly, we compose CCNOT from a set of five two-qubit gates [13], as shown in figure 1. The box with the bar on the right represents the square root of  $X$ ,

$$\sqrt{X} = \frac{1}{2} \begin{bmatrix} 1+i & 1-i \\ 1-i & 1+i \end{bmatrix}$$

and the box with the bar on the left its adjoint.

Section II reviews Shor's algorithm and the need for modular exponentiation, then summarizes the techniques we employ to accelerate modular exponentiation. The next subsection introduces the best-known existing modular exponentiation algorithms and several different adders. Section III begins by examining concurrency in the lowest level elements, the adders. This is followed by faster adders and additional techniques for accelerating modulo operations and exponentiation. Section IV shows how to balance these techniques and apply them to a specific architecture and set of constraints. We evaluate several complete algorithms for our architectural models. Specific gate latency counts, rather than asymptotic values, are given for 128 bits and smaller numbers.

## II. BASIC CONCEPTS

### A. Modular Exponentiation and Shor's Algorithm

Shor's algorithm for factoring numbers on a quantum computer uses the quantum Fourier transform to find the order  $r$  of a randomly chosen number  $x$  in the multiplicative group  $(\text{mod } N)$ . This is achieved by exponentiating  $x$ , modulo  $N$ , for a superposition of all possible exponents  $a$ . Therefore, efficient arithmetic algorithms to calculate modular exponentiation in the quantum domain are critical.

Quantum modular exponentiation is the evolution of the state of a quantum computer to hold

$$|\psi\rangle|0\rangle \rightarrow |\psi\rangle|x^\psi \bmod N\rangle \quad (1)$$

When  $|\psi\rangle$  is the superposition of all input states  $a$  up to a particular value  $2N^2$ ,

$$|\psi\rangle = \frac{1}{N\sqrt{2}} \sum_{a=0}^{2N^2} |a\rangle \quad (2)$$

The result is the superposition of the modular exponentiation of those input states,

$$\frac{1}{N\sqrt{2}} \sum_{a=0}^{2N^2} |a\rangle|0\rangle \rightarrow \frac{1}{N\sqrt{2}} \sum_{a=0}^{2N^2} |a\rangle|x^a \bmod N\rangle \quad (3)$$

Depending on the algorithm chosen for modular exponentiation,  $x$  may appear explicitly in a register in the quantum computer, or may appear only implicitly in the choice of instructions to be executed.

In general, quantum modular exponentiation algorithms are created from building blocks that do modular multiplication,

$$|\alpha\rangle|0\rangle \rightarrow |\alpha\rangle|\alpha\beta \bmod N\rangle \quad (4)$$

where  $\beta$  and  $N$  may or may not appear explicitly in quantum registers. This modular multiplication is built from blocks that perform modular addition,

$$|\alpha\rangle|0\rangle \rightarrow |\alpha\rangle|\alpha + \beta \bmod N\rangle \quad (5)$$

which, in turn, are usually built from blocks that perform addition and comparison.

$n$ -bit addition requires  $O(n)$  gates.  $n$ -bit multiplication (including modular multiplication) combines the convolution partial products (the one-bit products) of each pair of bits from the two arguments. This requires  $O(n)$  additions of  $n$ -bit numbers, giving a gate count of  $O(n^2)$ . Our exponentiation for Shor's algorithm requires  $2n$  multiplications, giving a total cost of  $O(n^3)$ .

Many of these steps can be conducted in parallel; in classical computer system design, the *latency* or *circuit depth*, the time from the input of values until the output becomes available, is as important as the total computational complexity. Our goal through the rest of the paper is to exploit parallelism, or concurrency, to shorten the total wall clock time to execute modular exponentiation, and hence Shor's algorithm.

### B. Notation and Techniques for Speeding Up Modular Exponentiation

In this paper, we will use  $N$  as the number to be factored, and  $n$  to represent its length in bits. For convenience, we will assume that  $n$  is a power of two, and the high bit is one.  $x$  is the random value, smaller than  $N$ , to be exponentiated, and  $|a\rangle$  is our superposition of exponents, with  $a < 2N^2$  so that the length of  $a$  is  $2n + 1$  bits.

When discussing circuit cost, the notation is  $(CCNOTs; CNOTs; NOTs)$  or  $(CNOTs; NOTs)$ . The values may be total gates or circuit depth (latency), depending on context. The notation is sometimes enhanced to show required concurrency and space,  $(CCNOTs; CNOTs; NOTs) \# (concurrency; space)$ .

When equations are subscripted with *AC*, *TC*, or *NTC*, the values are for the latency of the construct on that architecture. Equations without subscripts are for an abstract machine

assuming no concurrency, equivalent to a total gate count for the *AC* architecture.

$m$ ,  $g$ ,  $f$ ,  $p$ ,  $b$ , and  $s$  are parameters that determine the behavior of portions of our modular exponentiation algorithm.  $m$ ,  $g$ , and  $f$  are part of our carry-select/conditional-sum adder (sec. III C).  $p$  and  $b$  are used in our indirection scheme (sec. III F).  $s$  is the number of multiplier blocks we can fit into a chosen amount of space (sec. III D).

Here we summarize the techniques which are detailed in following subsections. Our fast modular exponentiation circuit is built using the following optimizations:

- Select correct qubit layout and subsequences to implement gates, then peephole optimize (no penalty) [14, 15, 16, 17, 18, 19, 20]
- Look for concurrency within addition/multiplication (no space penalty, maybe noise penalty) (secs. III A, III B)
- Select multiplicand using table/indirection (exponential classical cost, linear reduction in quantum gate count)([21], sec. III F)
- Do multiplications concurrently (linear speedup for small values, linear cost in space, small gate count increase; requires quantum-quantum (Q-Q) multiplier, as well as classical-quantum (C-Q) multiplier) (sec. III D).
- Move to e.g. carry-save adders ( $n^2$  space penalty for reduction to log time, increases total gate count)([5], sec. II C 3) conditional-sum adders (sec. III C), or carry-lookahead adders (sec. II C 4)
- Reduce modulo comparisons, only do subtract  $N$  on overflow (small space penalty, linear reduction in modulo arithmetic cost) (sec. III E)

### C. Existing Algorithms

There are many ways of building adders and multipliers, and choosing the correct one is a technology-dependent exercise [22]. Only a few classical techniques have been explored for quantum computation. The two most commonly cited modular exponentiation algorithms are those of Vedral, Barenco, and Ekert [2], which we will refer to as VBE, and Beckman, Chari, Devabhaktuni, and Preskill [3], which we will refer to as BCDP. BCDP and VBE both build multipliers from variants of carry-ripple adders, the simplest but slowest method. Zalka proposed a carry-select adder; we present our design for such an adder in detail in section III C. Draper *et al* have recently proposed a carry-lookahead adder, and Gossett a carry-save adder. Beauregard has proposed a circuit that operates primarily in the Fourier transform space.

Carry-lookahead (sec. II C 4), conditional-sum (sec. III C), and carry-save (sec. refsec:gossett) all reach  $O(\log n)$  performance for addition. Carry-lookahead and conditional-sum use more space than carry-ripple, but much less than carry-save.

$n$	VBE	BCDP
8	(34720; 43896; 497)	(18627; 5790; 7980)
16	(302400; 371952; 2017)	(186915; 44206; 72540)
32	(2.52E6; 3.06E6; 8129)	(1.64E6; 3.42E5; 6.17E5)
64	(2.06E7; 2.48E7; 32641)	(1.36E7; 2.68E6; 5.09E6)
128	(1.66E8; 2.00E8; 1.31E5)	(1.11E8; 2.12E7; 4.13E7)
512	(1.07E10; 1.29E10; 2.10E6)	(7.21E9; 1.35E9; 2.67E9)
1024	(8.58E10; 1.03E11; 8.39E6)	(5.79E10; 1.08E10; 2.14E10)
4096	(5.50E12; 6.60E12; 1.34E8)	(3.71E12; 6.87E11; 1.37E12)

TABLE I: Unoptimized gate counts for VBE and BCDP modular exponentiation algorithms for length  $n$ . Notation is (# of CCNOTs; # of CNOTs; # of NOTs).

However, carry-save adders can be combined into fast multipliers more easily. We will see in sec. III how to combine carry-lookahead and conditional-sum into the overall exponentiation algorithms.

#### 1. VBE Carry-Ripple

The VBE algorithm [2] builds full modular exponentiation from smaller building blocks: CARRY and SUM make a carry-ripple ADDER [33]; 5 ADDERs plus additional logic make ADDER MOD; successively  $n$  ADDER MODs plus a little extra logic make C-MULT MOD, and  $4n - 1$  calls to C-MULT MOD make the full exponentiation circuit ( $a$  is  $2n + 1$ , and each multiplication must be reversed to clear the input register). The full circuit requires  $7n + 1$  qubits of storage:  $2n + 1$  for  $a$ ,  $n$  for the other multiplicand,  $n$  for a running sum,  $n$  for the convolution products,  $n$  for a copy of  $N$ ,  $n$  for carries. The bulk of the time is spent in  $20n^2 - 5n$  ADDERs.

In this algorithm, the values to be added in, the convolution partial products of  $x^a$ , are programmed into a temporary register (combined with a superposition of  $|0\rangle$  as necessary) inside the C-MULT MOD block based on a control line and a data bit via appropriate CCNOT gates. Although the gates to set the value could be executed concurrently, propagating this control signal requires  $O(n)$  time on many technologies. Likewise, the modulus  $N$  appears and disappears repeatedly based on the overflow calculated in ADDER MOD.

$$\text{ADDER} = (4n - 4; 4n - 3; 0) \quad (6)$$

$$\begin{aligned} VEXP &= (4n - 1) * (\text{CMULTMOD}) + (0; 0; 1) \\ &= (4n - 1) * n * \text{ADDERMOD} \\ &= (4n - 1) * n * 5 * \text{ADDER} \\ &= (20n^2 - 5n) * \text{ADDER} \\ &= (20n^2 - 5n) * (4n - 4; 4n - 3; 0) \\ &= (80n^3 - 100n^2 + 20n; 96n^3 - 84n^2 + 15n; \\ &\quad 8n^2 - 2n + 1) \end{aligned} \quad (7)$$

Table I shows the number of gates needed for VBE, in its most abstract, least optimized form, calculated from equation 7. We have included only the minor optimizations from

knowing that the adder starts with a zero carry in, and the first inverse multiply in C-MULT MOD is unnecessary (see fig. 6 in [2]; we know that the register we are trying to clear contains 1 so it can be cleared with a single NOT). For the smallest values the accuracy of the table is questionable at best; Vandersypen optimized all the way down to a mere eight gates (2 CCNOT, 6 CNOT, 0 NOT) for exponentiating to factor the four-bit number 15 by using a number of arithmetic tricks (see fig. 5.34 in [14]).

## 2. BCDP Carry-Ripple

The BCDP algorithm (table I) is also based on a carry-ripple adder. It differs from VBE in that it more aggressively takes advantage of classical computation. However, for our purposes, this makes it harder to use some of the optimization techniques presented here. Beckman *et al* present several optimizations and tradeoffs of space and time, slightly complicating the analysis.

The exact sequence of gates to be applied is also dependent on the input values of  $N$  and  $x$ , making it less suitable for hardware implementation with fixed gates (e.g., in an optical system). The convolution partial products to be added into our running sum never explicitly appear in a register; they are implied in the set of gates chosen to execute. This can be viewed as a 1-bit version of our indirection scheme from section III F. For these reasons, this algorithm is more conservative with space than VBE. In the form we analyze, it requires  $5n + 3$  qubits, including  $2n + 1$  for  $|a\rangle$ .

The complete BCDP circuit consists of  $4n^2 - 6n + 2$  calls to the  $OADDN$  block, plus minor additional logic. The full, clean, modular BCDP adder,  $OADDN$ , is composed of two  $MADD$  adders and two  $XLT$  comparators. These are the only blocks in their construction which we need to consider. Borrowing from their equation 6.23,

$$\begin{aligned} EXPN(\text{avg}) = & (54n^3 - 127n^2 + 108n - 29; \\ & 10n^3 + 15n^2 - 38n + 14; \\ & 20n^3 - 38n^2 + 22n - 4) \end{aligned} \quad (8)$$

Note that this is Beckman *et al*'s average gate count, whereas the results we report in sec. IV B are for worst case.

## 3. Gossett Carry-Save and Carry-Ripple

Gossett's arithmetic is pure quantum, as opposed to the mixed classical-quantum of BCDP. Gossett does not provide a full modular exponentiation circuit, only adders, multipliers, and a modular adder based on the important classical techniques of *carry-save arithmetic* [5].

Gossett's carry-save adder, the important contribution of the paper, can run in  $O(\log n)$  time on  $AC$  and  $TC$  architectures. It will remain impractical for the foreseeable future due to the large number of qubits required; he estimates  $8n^2$  qubits for a full multiplier, which would run in  $O(\log^2 n)$ . It bears

further analysis because of its high speed and resemblance to standard fast classical multipliers.

Unfortunately, the paper's second contribution, Gossett's carry-ripple adder, as drawn in his figure 7, seems to be incorrect. His quantum majority gate (QMG) does not correctly undo the carry generated by his quantum full adder (QFA) when the carry is one and the sum is zero. His circuit is actually *backwards*; the QMGs should come before the QFAs, in which case his circuit optimizes to be almost identical to VBE.

## 4. Carry-Lookahead

Draper, Kutin, Rains, and Svore have recently proposed a carry-lookahead adder [23]. This method allows the latency of an adder to drop to  $O(\log n)$  for  $AC$  and  $TC$  architectures. The latency and storage of their adder is

$$\begin{aligned} QCLA_{AC} = & (4 \log_2 n + 3; 4; 2) \\ & \#(n; 4n - \log n - 1) \end{aligned} \quad (9)$$

The authors do not present a complete modular exponentiation circuit; we will use their adder in our algorithm E, which we evaluate only for  $AC$ . The large distances between gate operands make it appear that QCLA is unattractive for  $NTC$ .

## 5. Beauregard/Draper QFT-based Exponentiation

Beauregard has designed a circuit for doing modular exponentiation in only  $2n + 3$  qubits of space [24], based on Draper's clever method for doing addition on Fourier-transformed representations of numbers [25].

The depth of Beauregard's circuit is  $O(n^3)$ , the same as VBE and BCDP. However, we believe the constant factors on this circuit are very large; every modulo addition consists of four Fourier transforms and five Fourier additions.

The principle problem is the difficulty of testing for overflow in the Fourier representation. If this can be solved, it will become possible to perform the entire modular exponentiation in the Fourier transform space using Schönhage-Strassen and Beauregard.

# III. RESULTS: ALGORITHMIC OPTIMIZATIONS

We present our concurrent variants of VBE and BCDP, then move to faster adders. This is followed by methods for performing exponentiation concurrently, improving the modulo arithmetic, and indirection to reduce the number of quantum multiplications.

## A. Concurrent VBE

In figure 2, we show a three-bit concurrent version of the VBE ADDER. The dashed lines delineate the *CARRY*,

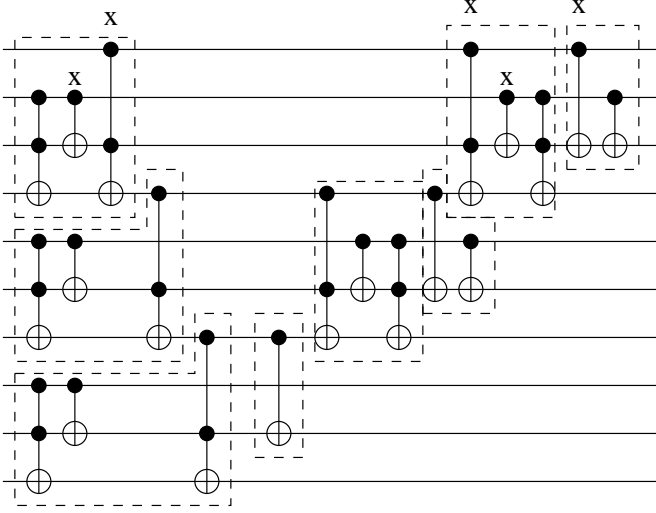


FIG. 2: Three-bit concurrent VBE ADDER, *AC* abstract machine. Gates marked with an 'x' can be deleted when the carry in is known to be zero.

*CARRY*, and *SUM* constructs. The lone gate in the center bottom is a *SUM* where one of the *CNOT* gates has cancelled with the *CNOT* at the center of the VBE ADDER. The gates marked with an 'x' can be optimized away, and the top qubit can be eliminated, because the top line is the "carry in" line, which is naturally zero. The gates are left in the figure for clarity. This figure shows that the delay of the concurrent ADDER is  $(3n - 3) * CCNOT + (2n - 3) * CNOT$ , or

$$ADDER_{AC} = (3n - 3; 2n - 3; 0) \quad (10)$$

a mere 25% reduction in latency compared to the unoptimized  $(4n - 4; 4n - 3; 0)$  of equation 6.

Adapting equation 7, the total circuit latency, minus a few small corrections that fall outside the ADDER block proper, is

$$\begin{aligned} VEXP_{AC} &= (20n^2 - 5n)ADDER_{AC} \\ &= (20n^2 - 5n)(3n - 3; 2n - 3; 0) \\ &= (60n^3 - 75n^2 + 15n; \\ &\quad 40n^3 - 70n^2 + 15n; 0) \end{aligned} \quad (11)$$

This equation is used to create the first entry in table III [34].

## B. Concurrent BCDP

Considering for the moment just the *MADD* block, the multiplexed, multi-bit adder for BCDP, we find a worst-case latency of  $(2n - 1; n - 1; 0)$ , as in figure 3. This is much better than the  $(4n; 2n; 2n)$  reported by BCDP. Significant optimization of the control lines resulted in some gates cancelling from the final circuit, and others being performed concurrently.

*XLT*, the comparator, which supports better concurrency than *MADD*, has a latency of  $(n; 1; 1)$  on *AC*. Since its dependency is from the high-order bits, rather than the low-order bits of adder carry, it does not pipeline with the adder effectively on an abstract machine.

The total latency of *OADDN* (worst case) is

$$\begin{aligned} OADDN_{AC} &= 2 * MADD_{AC} + 2 * XLT_{AC} \\ &= (6n - 2; 2n; 2) \end{aligned} \quad (12)$$

The latency of the total, concurrent circuit is approximately

$$\begin{aligned} EXPN_{AC} &= 2(2n - 1)(n - 1)OADDN_{AC} \\ &= (24n^3 - 44n^2 + 12n - 4; 8n^3 - 12n^2 + 8n; \\ &\quad 8n^2 - 12n + 4) \end{aligned} \quad (13)$$

on the *AC* architecture.

## C. Carry-Select and Conditional-Sum Adders

Carry-select adders concurrently calculate possible results without knowing the value of the carry in. Once the carry in becomes available, the correct output value is selected using a multiplexer (MUX). The type of MUX determines whether the behavior is  $O(\sqrt{n})$  or  $O(\log n)$ .

### 1. $O(\sqrt{n})$ Carry-Select Adder

The bits are divided into  $g$  groups of  $m$  bits each,  $n = gm$ . The adder block we will call *CSLA*, and the combined adder, *MUXes*, and adder undo to clean our ancillae, *CSLAMU*. The *CSLAs* are all executed concurrently, then the output *MUXes* are cascaded, as shown in figure 5. The first group may have a different size,  $f$ , than  $m$ , since it will be faster, but for the moment we assume they are the same.

Figure 4 shows a three-bit carry-select adder. This generates two possible results, assuming that the carry in will be zero or one. The portion on the right is a *MUX* used to select which carry to use, based on the carry in. All of the outputs without labels are ancillae to be garbage collected. It is possible that a design optimized for space could reuse some of those qubits; as drawn a full carry-select circuit requires  $5m - 1$  qubits to add two  $m$ -bit numbers.

The larger  $m$ -bit carry-select adder can be constructed so that its internal delay, as in a normal carry-ripple adder, is one additional *CCNOT* for each bit, although the total number of gates increases and the distance between gate operands increases.

The latency for the *CSLA* block is

$$CSLA_{AC} = (m; 2; 0) \quad (14)$$

Note that this is not a "clean" adder; we still have ancillae to return to the initial state.

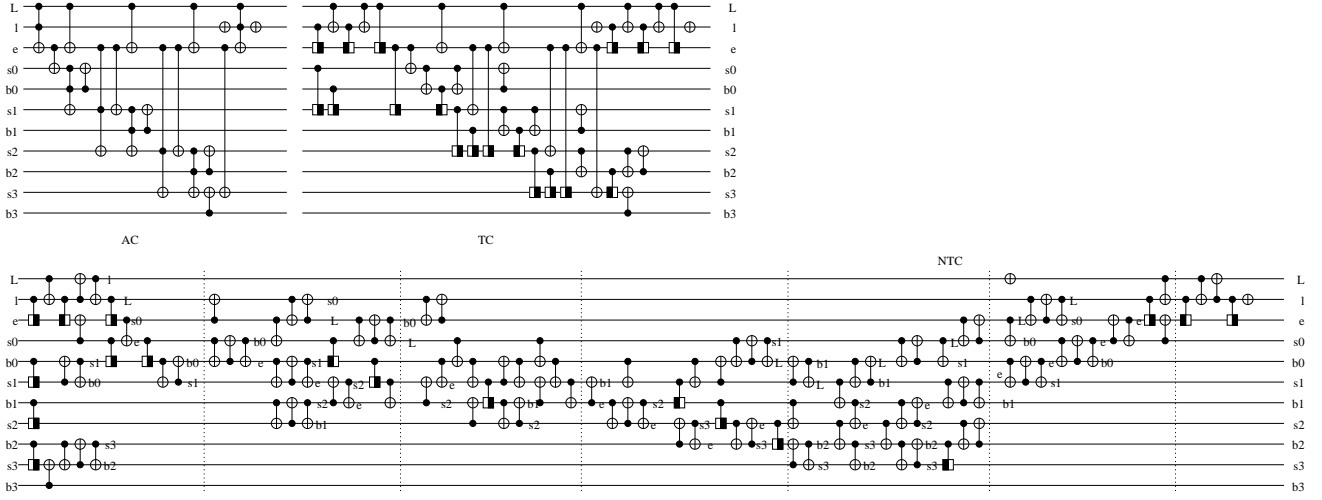
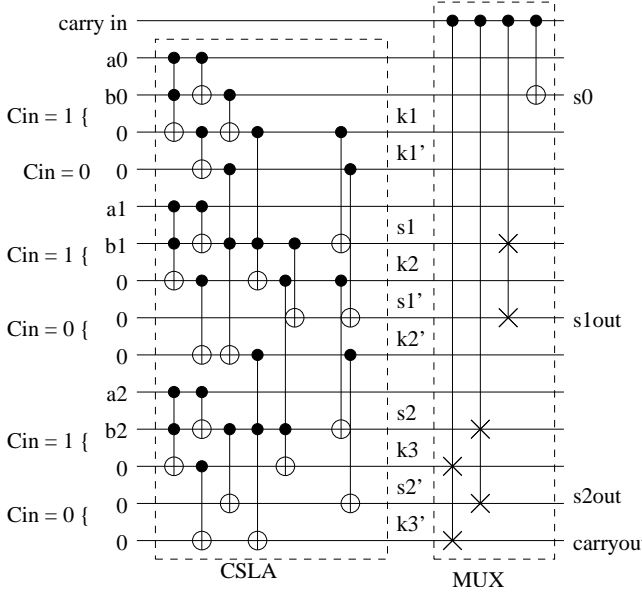
FIG. 3: Four-bit concurrent BCDP MADD (worst case, adding 1010 or 0101 depending on  $L$ )

FIG. 4: Three-bit carry-select adder with MUX

The problem for implementation will be creating an efficient MUX, especially on  $NTC$ . Figure 5 makes it clear that the total carry-select adder is only faster if the latency of MUX is substantially less than the latency of the full carry-ripple. It will be difficult for this to be more efficient than the single-CCNOT delay of the basic VBE carry-ripple adder on  $NTC$ . On  $AC$  and  $TC$ , it is certainly easy to see how the MUX can use a fanout tree consisting of more ancillae and CNOT gates to distribute the carry in signal, as suggested by Moore [7], allowing all MUX Fredkin gates to be executed concurrently. A full fanout requires an extra  $m$  qubits in each adder.

In order to unwind the ancillae to reuse them, the simplest approach is the use of CNOT gates to copy our result to another  $n$ -bit register, then a reversal of the circuitry. Counting the copy out for ancilla management, we can simplify the

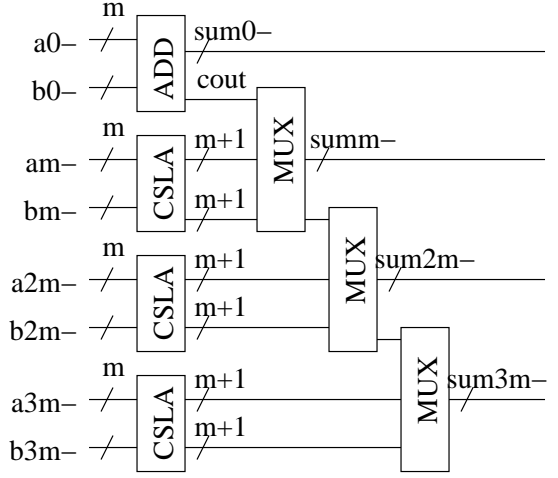


FIG. 5: Four-group carry-select adder

MUX to two CCNOTs and a pair of NOTs, as in figure 6.

The latency of the carry ripple from MUX to MUX (not qubit to qubit) can be arranged to give a MUX cost of  $(4g + 2m - 6; 0; 2g - 2)$ , as shown in figure 6. This cost can be accelerated somewhat by using a few extra qubits and “fanning out” the carry. For intermediate values of  $m$ , we will use a fanout of 4 on  $AC$  and  $TC$ , reducing the MUX latency to  $(4g + m/2 - 6; 2; 2g - 2)$  in exchange for 3 extra qubits in each group.

Our space used for the full, clean adder is  $(6m - 1)(g - 1) + 3f + 4g$  when using a fanout of 4.

The total latency of the CSLA, MUX, and the CSLA undo is

$$\begin{aligned}
 CSLAMU_{AC} &= 2CSLA_{AC} + MUX_{AC} \\
 &= 2(m; 2; 0) + (4g + m/2 - 6; 2; 2g - 2) \\
 &= (4g + 5m/2 - 6; 6; 2g - 2) \quad (15)
 \end{aligned}$$

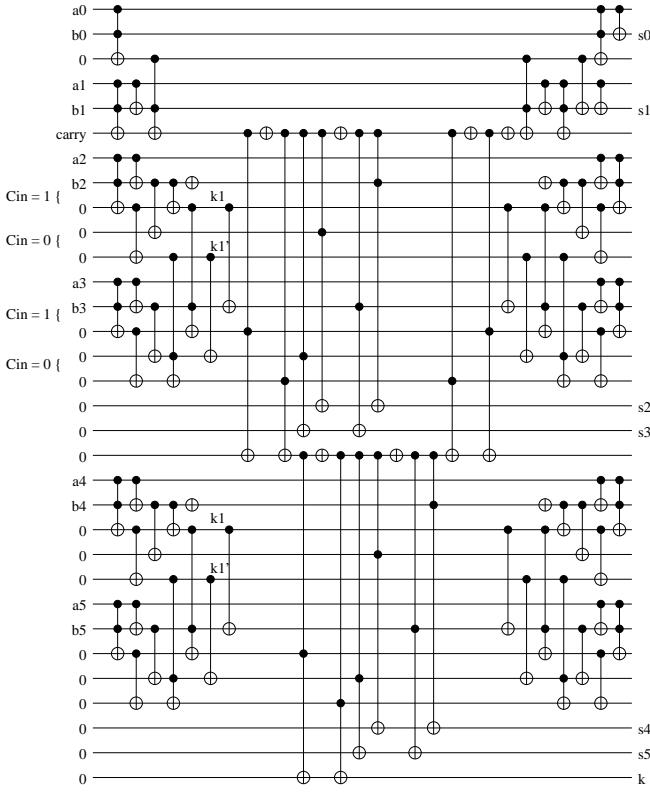


FIG. 6: Six-bit carry-select adder with carry out and MUX,  $m = 2$ ,  $g = 3$ , AC architecture. The central portion of the figure is the MUX, and the right hand portion is the undo to clean our ancillae.

Optimizing for AC, based on equation 15, the delay will be the minimum when  $m \sim \sqrt{8n/5}$ .

Zalka was the first to propose use of a carry-select adder, though he did not refer to it by name [6]. His analysis does not include an exact circuit, and his results differ slightly from ours.

## 2. $O(\log n)$ Conditional Sum Adder

As described above, the carry-select adder is  $O(m + g)$ , for  $n = mg$ , which minimizes to be  $O(\sqrt{n})$ . To reach  $O(\log n)$  performance, we must add a multi-level MUX to our carry-select adder. This structure is called a conditional sum adder. Rather than repeatedly choosing bits at each level of the MUX, we will create a multi-level distribution of MUX select signals, then apply them once at the end. Figure 7 shows only the carry signals for eight CSLA groups. The 'e' signals in the figure are our effective swap control signals. They are combined with a carry in signal to control the actual swap of variables. In a full circuit, a ninth group, the first group, will be a carry-ripple adder and will create the carry in; that carry in will be distributed concurrently in a separate tree.

The total adder latency will be

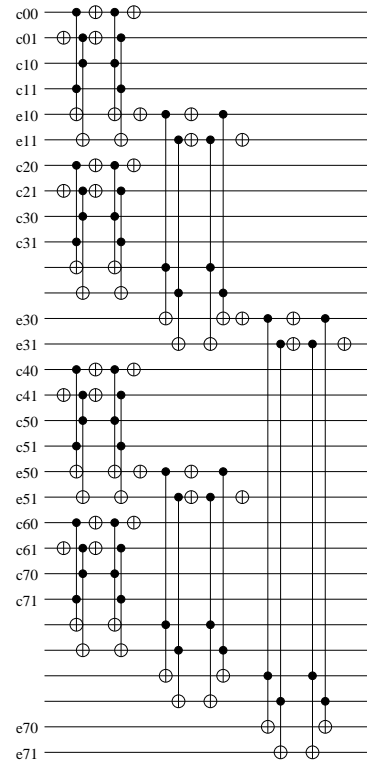


FIG. 7:  $O(\log n)$  MUX for conditional-sum adder, for  $g = 9$  (the first group is not shown). At each stage, the span of correct effective swap control lines 'e' doubles. After using the swap control lines, all but the last must be cleaned by reversing the circuit. Only the carry out lines from each  $m$ -qubit block are shown. Unlabeled lines are ancillae to be cleaned.

$$\begin{aligned}
 CSLALOM_{AC} &= 2 * CSLA_{AC} + \\
 &\quad (2 * \lceil \log_2(g-1) \rceil - 1) * (2; 0; 2) \\
 &\quad +(4; 0; 4) \\
 &= (2m + 4\lceil \log_2(g-1) \rceil + 2; 4; \\
 &\quad 4\lceil \log_2(g-1) \rceil + 2) \quad (16)
 \end{aligned}$$

For large  $n$ , this generally reaches a minimum for small  $m$ , which gives asymptotic behavior  $\sim 4 \log_2 n$ , the same as QCLA. CSLALOM is noticeably faster for small  $n$ , but requires more space.

The MUX uses  $\lceil 3(g-1)/2 \rceil - 2$  qubits in addition to the internal carries and the tree for dispersing the carry in. Our space used for the full, clean adder is  $(6m-1)(g-1) + 3f + \lceil 3(g-1)/2 - 2 + (n-f)/2 \rceil$ .

## D. Concurrent Exponentiation

Modular exponentiation is often drawn as a string of modular multiplications, but Cleve and Watrous pointed out that these can easily be parallelized, at linear cost in space [4]. We always have to execute  $2n$  multiplications; the goal is to do them in as few time-delays as possible.

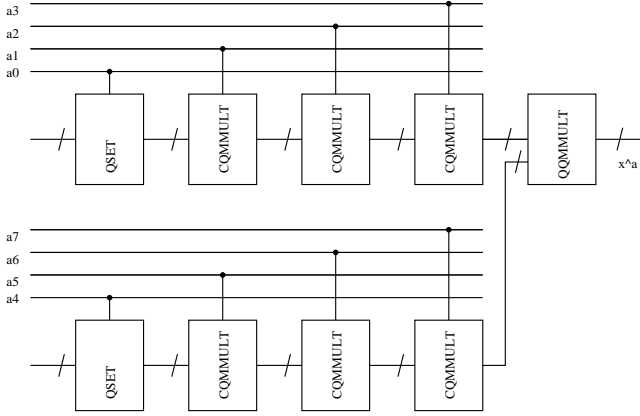


FIG. 8: Concurrent modular multiplication in modular exponentiation for  $s = 2$ . QSET simply sets the sum register to the appropriate value.

To go (almost) twice as fast, use two multipliers. For four times, use four. Naturally, this can be built up to  $n$  multipliers to multiply the necessary  $2n + 1$  numbers, in which case recombining the partial results requires  $\log_2 n$  quantum-quantum (Q-Q) multiplier latency times. The first unit in each chain just sets the register to the appropriate value if the control line is 1, otherwise, it leaves it as 1.

The VBE multiplier can easily be modified to support Q-Q multiplication; BCDP cannot. For the moment, however, we will assume that a Q-Q multiplier can be found that costs the same as a classical-quantum (C-Q) one. We will also assume that it is acceptable, as we combine these partial results, to leave the arguments in registers. We do not need the space for the Fourier transform to come, however, it may be necessary to disentangle the argument from the result for algorithmic purposes. If so, the cost of multi-multiplier exponentiation must be doubled to undo the arguments.

For  $s$  multipliers,  $s \leq n$ , each multiplier must combine  $t = \lfloor (2n+1)/s \rfloor$  or  $t+1$  numbers, using  $t-1$  or  $t$  multiplications (the first number being simply set into the running product register). The intermediate results from the multipliers are combined using  $\lceil \log_2 s \rceil$  Q-Q multiplications.

For a parallel version of VBE, the exact latency, including cases where  $ts \neq 2n + 1$ , is

$$\text{MULTS}_{VBE} = 2t + 1 + \lceil \log_2 (\lceil (s - 2n - 1 + ts)/4 \rceil + 2n + 1 - ts) \rceil \quad (17)$$

times the latency of our multiplier. For small  $s$ , this is  $O(n)$ ; for larger  $s$ ,

$$\lim_{s \rightarrow n} O(n/s + \log s) = O(\log n) \quad (18)$$

For a parallel version of BCDP, the exact latency, including cases where  $ts \neq 2n + 1$ , is

$$\text{MULTS}_{BCDP} = t + 1 + \lceil \log_2 (\lceil (s - 2n - 1 + ts)/4 \rceil + 2n + 1 - ts) \rceil \quad (19)$$

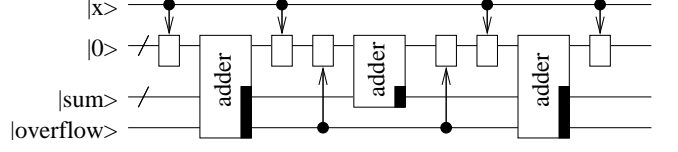


FIG. 9: More efficient modulo adder. The blocks with arrows set the register contents based on the value of the control line. The position of the black block indicates the running sum in our output.

times the latency of our multiplier. For BCDP, it is not necessary to undo the multiplication. The asymptotic behavior is the same.

### E. Reducing the Cost of Modulo Operations

VBE does a trial subtraction of  $N$  in each MOD ADD block; if that underflows,  $N$  is added back in to the total. This accounts for two of the five ADDER blocks and much of the extra logic. The last two of the five blocks are required to undo the overflow bit.

BCDP performs a direct comparison  $XLT$  to  $N$  to decide what value to add to the current sum, adding either  $x$  or  $2^n + x - N$ . The overflow wraps the register, rather than requiring extra adder blocks to subtract  $N$ . This is the source of much of BCDP's performance advantage compared to VBE, offset by its more complex block called  $OADDN$ , composed of  $MADD + XLT$ , doubled to clear the input register and overflow bit.

Figure 9 shows a more efficient modulo adder than VBE, based partly on ideas from BCDP and Gossett. It requires only three adder blocks, compared to five for VBE, to do one modulo addition. The first adder, in fact, need not be a complete adder, but, like BCDP's  $XLT$ , exists primarily to determine the overflow bit. We will assume that it is a complete adder. The first adder adds  $x^j$  to our running sum; the second conditionally adds  $2^n - x^j - N$  or 0, depending on the value of the overflow bit, arranging it so that the third addition of  $x^j$  will overflow and clear the overflow bit. The blocks pointed to by arrows are the addend register, whose value is set depending on the control lines.

Figure 9 uses  $n$  fewer bits than VBE's modulo arithmetic, as it does not require a register to hold  $N$ .

In a slightly different fashion, we can improve the performance of VBE by adding a number of qubits,  $p$ , to our result register, and postponing the modulo operation until later. This works as long as we don't allow the result register to overflow; we have a redundant representation of modulo  $N$  values, but that is not a problem at this stage of the computation.

The largest number that doesn't overflow for  $p$  extra qubits is  $2^{n+p} - 1$ ; the largest number that doesn't result in subtraction is  $2^{n+p-1} - 1$ . We want to guarantee that we always clear that high-order bit, so if we subtract  $bN$ , the most iterations we can go before the next subtraction is  $b$ .

The largest multiple of  $N$  we can subtract is  $\lfloor 2^{n+p-1}/N \rfloor$ . Since  $2^{n-1} < N < 2^n$ , the largest  $b$  we can allow is, in

general,  $2^{p-1}$ . For  $p > 2$ , when  $N$  is known to be close to  $2^{n-1}$ ,  $b$  may be a larger value, but still  $< 2^p$ .

The problem introduced by this scheme (avoided in figure 9 by using the third adder) is that we have no easy way to clear both the overflow bit and our addend register. We probably have no choice but to copy the result to a fresh register and reverse the computation to clear. This would use an extra  $n$  space and a total of  $2b + 1$  adders to perform  $b$  semi-modular additions. When using a carry-select adder that already copies out its result, it should be possible to do this without a space penalty.

For example, adding three qubits,  $p = 3$ , allows  $b = 4$ , reducing the 20 ADDER calls VBE uses for four additions to 9 ADDER calls, a 55% performance improvement. As  $p$  grows larger, the cost of the adjustment at the end of the calculation also grows and the additional gains are small. We must use  $3p$  adder calls at the end of the calculation to perform our final modulo operation. Calculations suggest that  $p$  of up to 10 or 11 is still faster.

The equation below shows the number of calls to our adder block necessary to make an  $n$ -bit modulo multiplier.

$$MMADDERCALLS = n * (2b + 1)/b \quad (20)$$

## F. Indirection

We have shown elsewhere that it is possible to build a table containing small powers of  $x$ , from which an argument to a multiplier is selected [21]. In exchange for adding storage space for  $2^w n$ -bit entries in a table, we can reduce the number of multiplications necessary by a factor of  $w$ . This appears to be attractive for small values of  $w$ , such as 2 or 3.

In our prior work, we proposed using a large quantum memory, or a quantum-addressable classical memory (QACM) [26]. Here we show that the quantum storage space need not grow; we can implicitly perform the lookup by choosing which gates to apply while adding. This is best done if the addition algorithm uses a temporary register to hold the addend, rather than performing each bit addition using implied values. In figure 10, we show the setting and resetting of the argument for  $w = 2$ , where the arrows indicate CCNOTs to set the appropriate bits of the 0 register to 1. The actual implementation can use a calculated enable bit to reduce the CCNOTs to CNOTs. Only one of the values  $a_0, a_1, a_2$ , or  $a_3$  will be enabled, based on the value of  $|x_1x_0\rangle$ .

The setting of this input register may require propagating  $|a\rangle$  or the enable bit across the entire register (true in VBE as well as with this indirection, and similar in BCDP) [35]. Use of a few extra qubits ( $2^{w-1}$ ) will allow the several setting operations to propagate in a tree. If a carry-ripple adder is used, the setting and unsetting may even be pipelined with the adder, reducing total latency.

$$ARGSET_{AC} = \begin{cases} 2^w(1; 0; 1) = (4; 0; 4) & w = 2 \\ 2^w(3; 0; 1) & w = 3, 4 \end{cases} \quad (21)$$

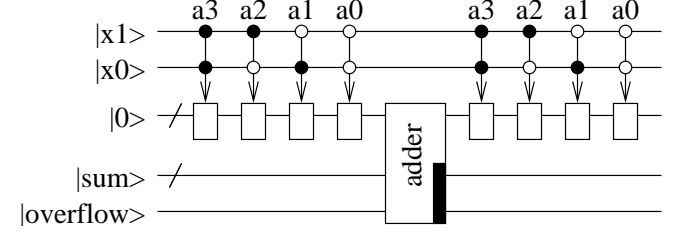


FIG. 10: Implicit Indirection. The arrows pointing to blocks indicate the setting of the addend register based on the control lines. This sets the addend from a table stored in classical memory, reducing the number of quantum multiplications by a factor of  $w$  in exchange for  $2^w$  argument setting operations.

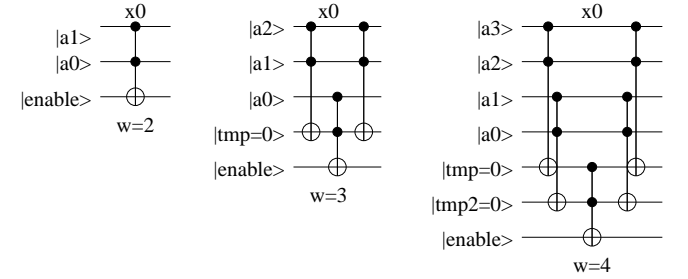


FIG. 11: AC argument setting for indirection for different values of  $w$ . For the  $w = 4$  case, the two CCNOTs on the left can be executed concurrently, as can the two on the right, for a total latency of 3.

For  $w = 2$  and  $w = 3$ , we calculate that setting the argument adds  $(4; 0; 4) \# (4, 5)$  and  $(24; 0; 8) \# (8, 9)$ , respectively, to the latency, concurrency and storage of each adder. We create separate enable signals for each of the  $2^w$  possible arguments and pipeline flowing them across the register to set the addend bits. We consider this cost only when using indirection. Figure 11 shows circuits for  $w = 2, 3, 4$ . These are based on the methods of Barenco *et al* [13], adapted for the fastest concurrent execution.

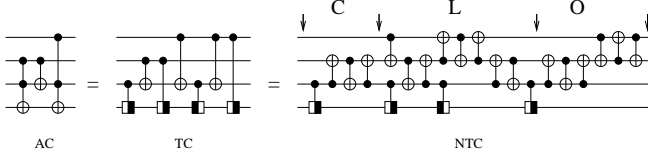
Adapting equation 17 to both indirection and concurrent multiplication, we have a total latency for our circuit, in multiplier calls, of

$$IMULTS = 2t + 1 + \lceil \log_2(\lceil (s-2n-1+ts)/4 \rceil + 2n+1-ts) \rceil \quad (22)$$

where  $t = \lfloor \lceil (2n+1)/w \rceil / s \rfloor$ .

## IV. EXAMPLE: EXPONENTIATING A 128-BIT NUMBER

In this section, we combine these techniques into complete algorithms and examine the performance of modular exponentiation of a 128-bit number. We assume the primary engineering constraint is the available number of qubits. In section III D we showed that using twice as much space can almost double our speed, essentially linearly until the log term begins to kick in. Thus, in managing space tradeoffs, this will be our standard; any technique that raises performance by more than a factor of  $c$  in exchange for  $c$  times as much space

FIG. 12: VBE CARRY for  $AC$ ,  $TC$ , and  $NTC$ 

will be used preferentially to parallel multiplication. Carry-select adders (sec. III C) easily meet this criterion, being perhaps six times faster for less than twice the space.

Algorithm **A** is our best effort in almost the same space as the original VBE algorithm,  $7n$ , adding only 9 bits to support indirection. Algorithm **B** uses  $100n$  space, and is tuned for architecture  $AC$  or  $TC$ . Algorithm **C** uses  $100n$  space, and is tuned for  $NTC$ . Algorithm **D** uses  $100n$  space and our conditional-sum adder. Algorithm **E** uses  $100n$  space and the carry-lookahead adder  $QCLA$ . Parameters for these algorithms are shown in table II, and results are shown in table III. The performance ratios are based only on the CCNOT gate count for  $AC$ , and only on the CNOT gate count for  $TC$  and  $NTC$ .

#### A. VBE and $100n$ VBE

On  $AC$ , the concurrent VBE ADDER is  $(3n - 3; 2n - 3; 0) = (381; 253; 0)$  for 128 bits. This is the value we use in the concurrent VBE line in table III. This will serve as our best baseline time for comparing the effectiveness of more drastic algorithmic surgery.

Inserting figure 1 directly into the VBE CARRY block increases the gate count from three to eleven. Optimizing those gates leaves us with seven, as shown in figure 12. Of those seven, three can be executed concurrently with other gates when cascaded CARRYs are done, leaving a latency of four. The total circuit depth of the VBE ADDER on a  $TC$  architecture is

$$ADDER_{TC} = (12n - 10; 0) \# (2; 3n + 1) \quad (23)$$

or  $(1526; 0) \# (2; 385)$  for 128 bits.

$$\begin{aligned} VEXP_{TC} &= (20n^2 - 5n) ADDER_{TC} \\ &= (20n^2 - 5n)(12n - 10; 0) \\ &= (240n^3 - 260n^2 + 50n; 0) \end{aligned} \quad (24)$$

Figure 12 also shows the same circuit, adapted to  $NTC$ . The four gates in the area marked “C” can be run concurrently during the add, the nine gate times in “L” are the core latency, and the six in “O” (the remaining SWAP operations) will be eliminated during optimization.

Figure 13 shows a fully optimized, concurrent, but otherwise unmodified version of the VBE ADDER for three bits on

a neighbor-only machine ( $NTC$  architecture), with the gates marked ‘x’ in figure 2 eliminated. The latency is

$$ADDER_{NTC} = (20n - 15; 0) \# (2; 3n + 1) \quad (25)$$

or 45 gate times for the three-bit adder. A 128-bit adder will have a latency of  $(2545; 0)$ . The diagram shows a concurrency level of three, but simple adjustment of execution time slots can limit that to two for any  $n$ , with no latency penalty.

The unmodified full VBE modular exponentiation algorithm, consists of  $20n^2 - 5n = 327040$  ADDER calls plus minor additional logic.

$$\begin{aligned} VEXP_{NTC} &= (20n^2 - 5n) ADDER_{NTC} \\ &= (20n^2 - 5n)(20n - 15; 0) \\ &= (400n^3 - 400n^2 + 75n; 0) \end{aligned} \quad (26)$$

The line for VBE  $100n$  is the same algorithm, unmodified except for parallel multiplication. The VBE multiplier uses  $5n + 1 = 641$  qubits of space, plus a single  $2n + 1 = 257$ -qubit copy of  $|a\rangle$  that can be shared among all multipliers. We can fit 19 multipliers into our  $100n = 12800$  allotted space, multiplying 13 or 14 numbers each. Using equation 17, we see that the latency is 31 multiplier calls. This compares to a cost of 511 multiplier calls without the parallelism.

#### B. BCDP and $100n$ BCDP

Figure 3 shows a worst-case four-bit BCDP  $MADD$  for  $AC$ ,  $TC$ , and  $NTC$ . The latency for  $TC$  is  $(24; 1)$  and for  $NTC$  is  $(64; 1)$ . The 40 extra gates in  $NTC$  are strictly for communications purposes, to be optimized or eliminated when possible. The circuit shown may not be optimal, but we believe it to be representative of the approach that will be used as the circuit is scaled up to larger  $n$ .  $TC$  latency is  $(4n + 8; 1)$ . For  $NTC$ , generalizing from this figure is difficult, but based on the placement of the square root of  $X$  gates, we estimate a latency of  $(23n - 28; 1)$  if the full circuit is used. This can be reduced to  $(17n - 4; 1)$  once the  $L$  and  $e$  variables’ return swap chain is optimized out, as will happen when the  $MADD$  and  $MADD^{-1}$  blocks are combined while making  $OADDN$ . Therefore, we will use  $(17n - 4; 1)$  as our  $MADD$  latency for further calculations for  $NTC$ . This compares to a latency of  $(2n - 1; n - 1; 0)$  for  $AC$ .

For  $XLT$ , we will assume a latency of  $(4n; 4)$  for  $TC$  and a SWAP-heavy  $(11n; 0)$  for  $NTC$ . This gives a total latency of

$$\begin{aligned} OADDN_{TC} &= 2(MADD_{TC} + XLT_{TC}) \\ &= (16n - 16; 10) \end{aligned} \quad (27)$$

for  $TC$  and

$$OADDN_{NTC} = (56n - 8; 2) \quad (28)$$

algorithm	adder	modulo	indirect	multipliers ( $s$ )	space	concurrency
concurrent VBE	VBE	VBE	N/A	1	897	2
concurrent BCDP	BCDP	BCDP	N/A	1	643	2
conc. VBE (100n)	VBE	VBE	N/A	19	12435	$2 * 19 = 38$
conc. BCDP (100n)	BCDP	BCDP	N/A	32	12609	$2 * 32 = 64$
algorithm <b>A</b>	VBE	fig. 9	$w = 3$	1	778	10
algorithm <b>B</b>	CSLA( $m = 16$ )	$p = 10, b = 512$	$w = 3$	14	12745	$114 * 14 = 1596$
algorithm <b>C</b>	VBE	$p = 9, b = 256$	$w = 4$	16	10929	$(16 + 2) * 16 = 288$
algorithm <b>D</b>	CSLALOM( $m = 4$ )	$p = 11, b = 1024$	$w = 2$	12	11969	$126 * 12 = 1512$
algorithm <b>E</b>	QCLA	$p = 10, b = 512$	$w = 2$	16	12657	$128 * 16 = 2048$

TABLE II: Parameters for our algorithms, chosen for 128 bits.

algorithm	<i>AC</i>		<i>TC</i>		<i>NTC</i>	
		gates	perf.		gates	perf.
concurrent VBE	( $1.25e + 08$ ; $8.27e + 07$ ; $0.00e + 00$ )	1.0	( $4.99e + 08$ ; $0.00e + 00$ )	1.0	( $8.32e + 08$ ; $0.00e + 00$ )	1.0
concurrent BCDP	( $4.96e + 07$ ; $1.66e + 07$ ; $1.30e + 05$ )	2.5	( $1.32e + 08$ ; $6.48e + 05$ )	3.8	( $4.64e + 08$ ; $1.30e + 05$ )	1.8
100n VBE	( $7.56e + 06$ ; $5.02e + 06$ ; $0.00e + 00$ )	16.5	( $3.03e + 07$ ; $0.00e + 00$ )	16.5	( $5.05e + 07$ ; $0.00e + 00$ )	16.5
100n BCDP	( $2.53e + 06$ ; $8.45e + 05$ ; $6.60e + 03$ )	49.3	( $6.71e + 06$ ; $3.30e + 04$ )	74.4	( $2.36e + 07$ ; $6.60e + 03$ )	35.2
algorithm A	( $2.66e + 07$ ; $1.66e + 07$ ; $5.25e + 05$ )	4.7	( $1.07e + 08$ ; $5.25e + 05$ )	4.7	( $1.77e + 08$ ; $5.25e + 05$ )	4.7
algorithm B	( $3.71e + 05$ ; $3.30e + 04$ ; $9.06e + 04$ )	335.9	( $1.38e + 06$ ; $9.48e + 04$ )	360.4	( $1.71e + 07$ ; $1.03e + 05$ )	48.8
algorithm C	( $1.22e + 06$ ; $7.21e + 05$ ; $4.51e + 04$ )	102.1	( $4.89e + 06$ ; $4.51e + 04$ )	102.1	( $8.11e + 06$ ; $4.51e + 04$ )	102.7
algorithm D	( $2.19e + 05$ ; $2.57e + 04$ ; $1.67e + 05$ )	569.8		N/A	N/A	N/A
algorithm E	( $1.71e + 05$ ; $1.96e + 04$ ; $2.93e + 04$ )	727.2		N/A	N/A	N/A

TABLE III: Latency to factor a 128-bit number for various architectures and choices of algorithm. *AC*, abstract concurrent architecture. *TC*, two-qubit gate, concurrent architecture. *NTC* neighbor-only, two-qubit gate, concurrent architecture. perf, performance relative to VBE algorithm for that architecture, based on CCNOTs for *AC* and CNOTs for *TC* and *NTC*.

for *NTC*.

BCDP 100n is for  $s = 32$  multipliers. Using equation 19, we calculate a latency of 13 multipliers.

For  $n = 128$ , BCDP uses  $2(n - 1)OADDN = 254 * OADDN$  to make a multiplier.  $OADDN = (2064; 10)$  for *TC*,  $(7160; 2)$  for *NTC*. The total latency is

$$EXPN100N_{AC} = MULTS_{BCDP} * (2(n - 1)) * OADDN_{AC} \quad (29)$$

and similarly for *NTC*.

### C. Algorithm A

Algorithm **A** is similar to VBE, but uses indirection and the modulo arrangement of figure 9. We will use an indirect of  $w = 3$ , charging  $(24; 0; 8) \# (8, 9)$  to our total adder latency for argument setting for *AC*. Figure 14 shows that the latency for creating the enable for argument setting for  $w = 3$  (and  $w = 4$ ) is

$$ARGSET_{TC} = 2^w(12; 1) = (96; 8) \quad (30)$$

$$ARGSET_{NTC} = 2^w(19; 1) = (152; 8) \quad (31)$$

$$\begin{aligned} AEXP &= (2 * \lceil (2n + 1)/w \rceil - 1) * CMULTMOD \\ &= (2 * \lceil (2n + 1)/w \rceil - 1) * n * ADDERMOD \\ &= 3n * (2 * \lceil (2n + 1)/w \rceil - 1) \\ &\quad * (ADDER + ARGSET) \end{aligned} \quad (32)$$

$$\begin{aligned} AEXP_{AC} &= 3n * (2 * \lceil (2n + 1)/w \rceil - 1) \\ &\quad * ((3n - 3; 2n - 3; 0) + (24; 0; 8)) \end{aligned} \quad (33)$$

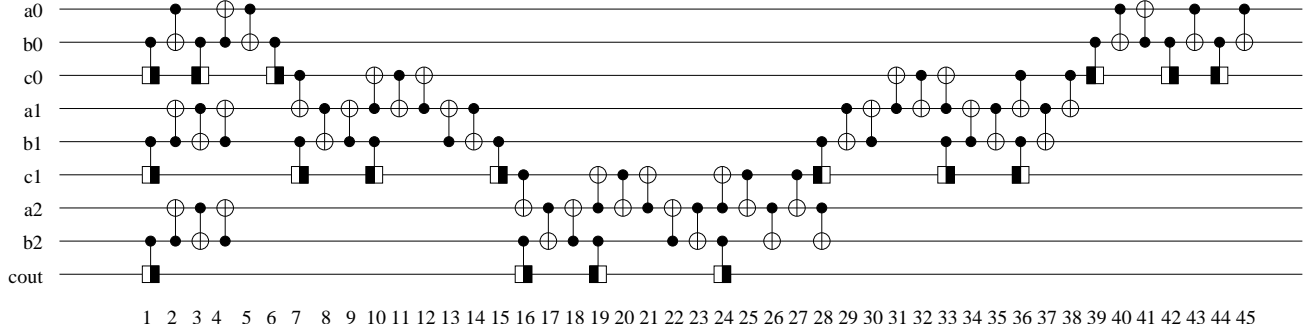
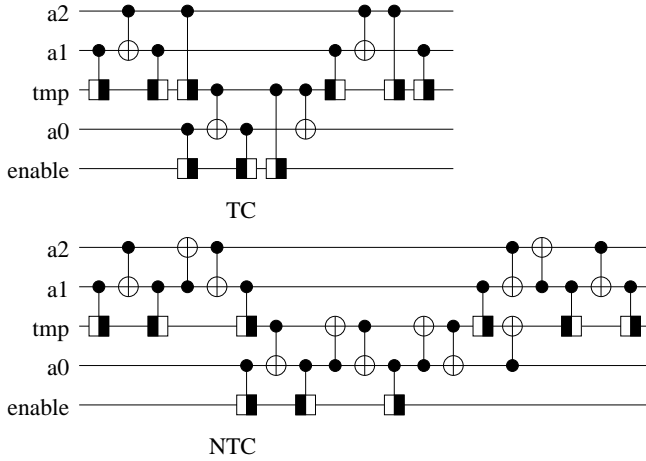
$$\begin{aligned} AEXP_{TC} &= 3n * (2 * \lceil (2n + 1)/w \rceil - 1) \\ &\quad * ((12n - 10; 0) + (96; 8)) \end{aligned} \quad (34)$$

$$\begin{aligned} AEXP_{NTC} &= 3n * (2 * \lceil (2n + 1)/w \rceil - 1) \\ &\quad * ((20n - 15; 0) + (152; 8)) \end{aligned} \quad (35)$$

Algorithm **A** uses

$$\begin{aligned} AEXP_{SPACE} &= 3n + 2^w + 1 + n + 2n + 1 \\ &= 6n + 2^w + 2 \end{aligned} \quad (36)$$

qubits of storage.

FIG. 13: Optimized, concurrent three bit VBE ADDER,  $NTC$ FIG. 14: Enable signal creation for argument setting for  $w = 3$  indirection, for  $TC$  and  $NTC$  architectures.

#### D. Algorithm B

The overall structure of algorithm **B** is similar to VBE, with our carry-select adders instead of the VBE carry-ripple, and our improvements in indirection and modulo.

Figure 15 shows three-bit carry-select adders for  $TC$  and  $NTC$  architectures. The gates in dotted boxes are to be executed concurrently. For  $TC$ , the latency is  $(3m + 3; 0)$ . For  $NTC$ , the latency is  $(12m + 9; 0)$  as drawn, but portions of that may be optimized away when combined with the MUX and the inverse adder. We will use an effective latency of  $(12m + 9; 0)$ . For our 128-bit circuit, we have chosen the group size  $m = 16$  giving  $g = 8$  groups, so we have  $(51; 0)$  and  $(201; 0)$ , respectively.

For  $TC$ , the bottleneck in the MUX is use of the carry. As mentioned in section III C, we will use a fanout of 4 on  $TC$ . The group-to-group latency is  $(2g - 3)(7; 1) + (3; 0)$ . The intra-group latency is, for a fanout of 4,  $(2; 0)$  to fanout the carry and  $(2; 0)$  to unset at the end, plus  $(m/4)(10; 0) + (0; 2)$  for the action gates, giving

$$\begin{aligned} MUX_{TC} &= (2g - 3)(7; 1) + (3; 0) \\ &\quad + (4; 0) + (m/4)(10; 0) + (0; 2) \\ &= (14g + (5/2)m - 14; 2g - 1) \end{aligned} \quad (37)$$

$$\begin{aligned} CSLAMU_{TC} &= 2CSLA_{TC} + MUX_{TC} \\ &= 2(3m + 3; 0) \\ &\quad + (14g + (5/2)m - 14; 2g - 1) \\ &= (8m + (1/2)m + 14g - 8; \\ &\quad 2g - 1) \end{aligned} \quad (38)$$

An efficient MUX for  $NTC$  is difficult to design. Our best effort [36] will still use our fanout bits, as the CCNOT gates add a significant delay that can be alleviated by hurrying a copy of the carry in down the chain.

$$\begin{aligned} MUX_{NTC} &= 2 * 5(n - m)(3; 0) + (2g - 3)(13; 1) \\ &\quad + m/4 * (13; 1) \\ &= (30n - 30m + 13m/4 + 26g - 39; \\ &\quad 2g - 3 + m/4) \end{aligned} \quad (39)$$

$$\begin{aligned} CSLAMU_{NTC} &= 2CSLA_{NTC} + MUX_{NTC} \\ &= 2(12m + 9; 0) \\ &\quad + (30n - 30m + 13m/4 + 26g - 39; \\ &\quad 2g - 3 + m/4) \\ &= (30n - 9m + m/4 + 26g - 21; \\ &\quad 2g - 3 + m/4) \end{aligned} \quad (40)$$

The large number of extra qubits for carry-select impose a significant communications penalty on  $NTC$ , with 80% of the latency in the MUX. This is more than the latency for the VBE ADDER, but consumes quite a bit more space, so we conclude that carry-select is impractical on  $NTC$  machines.

Using the faster modulo with  $p = 4$  lets us use 9 adder calls for each four additions, or  $MMADDERCALLS = 288$  adder calls in a 128-bit multiplier.

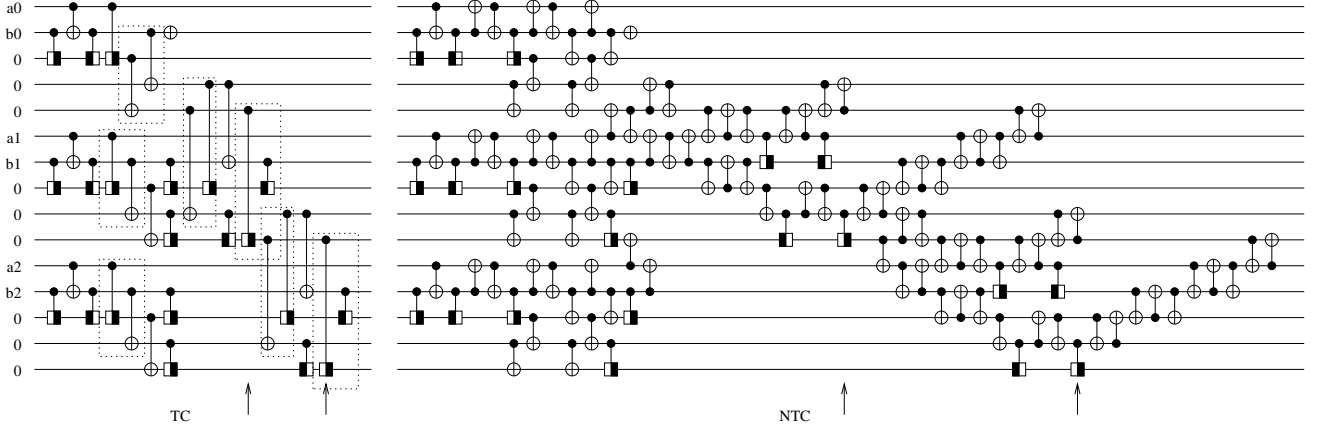


FIG. 15: Three-bit carry-select adders for  $TC$  and  $NTC$  architectures. Latencies of the adders can be calculated by comparing placement of the square root of  $X$  gates for successive qubits, marked with arrows.

We will use an indirect of  $w = 3$ , giving  $(100; 8; 38)$  for  $AC$ . For  $TC$  we get  $(478; 38)$  and  $(3194; 26)$  for  $NTC$ .

Our total space needs are  $((6m-1)(g-1)+3f+3g)+(2^w+1)+p = 764$  qubits for each adder, plus another register of size  $n$  as a temporary register in each multiplier (which holds the convolution products), plus  $2n$  to hold one copy of  $|a\rangle$ . In  $100n = 12800$  space, we can hold 14 multipliers. Plugging these values into equation 22, we find  $IMULTS = 16$ .

$$BEXP = IMULTS * MMADDERCALLS * (CSLAMU + ARGSET) + 3p * CSLAMU \quad (41)$$

Letting  $b = 2^{p-1}$  and  $t = \lceil (2n+1)/w \rceil / s$ ,

$$BEXP_{AC} = 2t + 1 + \lceil \log_2(\lceil (s-2n-1+ts)/4 \rceil + 2n+1-ts) \rceil * n * (2b+1)/b * ((4g+5m/2-6; 8; 2g-2) + (24; 0; 8)) + 3p * (4g+5m/2-6; 8; 2g-2) \quad (42)$$

$$BEXP_{TC} = 2t + 1 + \lceil \log_2(\lceil (s-2n-1+ts)/4 \rceil + 2n+1-ts) \rceil * n * (2b+1)/b * ((8m+(1/2)m+14g-8; 2g-1) + (96; 8)) + 3p * (8m+(1/2)m+14g-8; 2g-1) \quad (43)$$

$$BEXP_{NTC} = 2t + 1 + \lceil \log_2(\lceil (s-2n-1+ts)/4 \rceil + 2n+1-ts) \rceil * n * (2b+1)/b * ((30n-9m+m/4+26g-21; 2g-3+m/4) + (152; 8)) + 3p * (30n-9m+m/4+26g-21; 2g-3+m/4) \quad (44)$$

Algorithm **B** uses a total of

$$BEXP_{SPACE} = s * (CSLAMU_{SPACE} + 2^w + 1 + p + n) + 2n + 1 = s * ((6m-1) * (g-1) + 3m + 4g + 2^w + 1 + p + n) + 2n + 1 = s * (7n - 3m + 3g + 2^w + 2 + p) + 2n + 1 \quad (45)$$

qubits of storage.

### E. Algorithm C

Algorithm **C** is our attempt to optimize for  $NTC$ . We have replaced the carry-select adder in algorithm **B** with the concurrent VBE ADDER.

$$CEXP = IMULTS * MMADDERCALLS * (ADDER + ARGSET) + 3p * ADDER \quad (46)$$

$$CEXP_{AC} = 2t + 1 + \lceil \log_2(\lceil (s-2n-1+ts)/4 \rceil + 2n+1-ts) \rceil * n * (2b+1)/b * ((3n-3; 2n-3; 0) + (48; 0; 16)) + 3p * (3n-3; 2n-3; 0) \quad (47)$$

$$\begin{aligned}
CEXP_{TC} = & 2t + 1 + \lceil \log_2(\lceil (s - 2n - 1 + ts)/4 \rceil \\
& + 2n + 1 - ts) \rceil * n * (2b + 1)/b \\
& * ((12n - 10; 0) + (192; 16)) \\
& + 3p * (12n - 10; 0)
\end{aligned} \tag{48}$$

$$\begin{aligned}
CEXP_{NTC} = & 2t + 1 + \lceil \log_2(\lceil (s - 2n - 1 + ts)/4 \rceil \\
& + 2n + 1 - ts) \rceil * n * (2b + 1)/b \\
& * ((20n - 15; 0) + (304; 16)) \\
& + 3p * (20n - 15; 0)
\end{aligned} \tag{49}$$

Algorithm **C** uses a total of

$$\begin{aligned}
CEXP_{SPACE} = & s * (ADDERSPACE \\
& + 2^w + 1 + p + n + n) + 2n + 1 \\
= & s * (3n + 2^w + 1 + p + 2n) \\
& + 2n + 1 \\
= & s * (5n + 2^w + 1 + p) + 2n + 1
\end{aligned} \tag{50}$$

qubits of storage.

#### F. Algorithm D

Other than replacing the carry-select adder with the conditional sum adder CSLALOM, this algorithm is similar to **B**. As we do not consider CSLALOM to be a good candidate for an algorithm for *NTC*, we evaluate only for *AC*. Algorithm **D** is the fastest algorithm for  $n = 8$  and  $n = 16$ .

$$\begin{aligned}
DEXP = & IMULTS * MMADDERCALLS \\
& * (CSLALOM + ARGSET) \\
& + 3p * CSLALOM
\end{aligned} \tag{51}$$

Letting  $t = \lceil \lceil (2n + 1)/w \rceil / s \rceil$ ,

$$\begin{aligned}
DEXP_{AC} = & 2t + 1 + \lceil \log_2(\lceil (s - 2n - 1 + ts)/4 \rceil \\
& + 2n + 1 - ts) \rceil * n * (2b + 1)/b \\
& * ((2m + 4\lceil \log_2(g - 1) \rceil + 2; 4; \\
& 4\lceil \log_2(g - 1) \rceil + 2) + (4; 0; 4)) \\
& + 3p * (2m + 4\lceil \log_2(g - 1) \rceil + 2; 4; \\
& 4\lceil \log_2(g - 1) \rceil + 2)
\end{aligned} \tag{52}$$

$$\begin{aligned}
DEXP_{SPACE} = & s * (CSLALOM_{SPACE} \\
& + 2^w + 1 + p + n) + 2n + 1 \\
= & s * ((6m - 1) * (g - 1) + 3m \\
& + \lceil 3(g - 1)/2 - 2 + (n - m)/2 \rceil \\
& + 2^w + 1 + p + n) + 2n + 1 \\
= & s * (7n - 3m - g + 2^w + p \\
& + \lceil 3(g - 1)/2 - 2 + (n - m)/2 \rceil) \\
& + 2n + 1
\end{aligned} \tag{53}$$

#### G. Algorithm E

Algorithm **E** uses the carry-lookahead adder QCLA in place of the conditional-sum adder CSLALOM. Although CSLALOM is slightly faster than QCLA, its significantly larger space consumption means that in our  $100n$  fixed-space analysis, we can fit in 16 multipliers using QCLA, compared to only 12 using CSLALOM. This allows the overall algorithm **E** to be 28% faster than **D** for 128 bits.

$$\begin{aligned}
EEXP = & IMULTS * MMADDERCALLS \\
& * (QCLA + ARGSET) + 3p * QCLA
\end{aligned} \tag{54}$$

$$\begin{aligned}
EEXP_{AC} = & 2t + 1 + \lceil \log_2(\lceil (s - 2n - 1 + ts)/4 \rceil \\
& + 2n + 1 - ts) \rceil * n * (2b + 1)/b \\
& * ((4\log_2 n + 3; 4; 2) + (4; 0; 4)) \\
& + 3p * (4\log_2 n + 3; 4; 2)
\end{aligned} \tag{55}$$

$$\begin{aligned}
EEXP_{SPACE} = & s * (QCLA_{SPACE} \\
& + 2^w + 1 + p + 2n) + 2n + 1 \\
= & s * (4n - \lceil \log_2(n) \rceil - 1 \\
& + 2^w + 1 + p + 2n) + 2n + 1 \\
= & s * (6n - \lceil \log_2(n) \rceil + 2^w + p) \\
& + 2n + 1
\end{aligned} \tag{56}$$

#### H. Smaller $n$ and Different Space

Figure 16 shows the execution times of our four fastest algorithms for  $n$  from eight to 128 bits. Algorithm **D**, using CSLALOM, is the fastest for eight and 16 bits, while **E**, using QCLA, is fastest for larger values. The latency of 1072 for 8 bits is 32 times faster than concurrent VBE, achieved with  $60n = 480$  qubits of space.

Figure 17 shows the execution times for 128 bits for various amounts of available space. All of our algorithms have reached a minimum by  $240n$  space (roughly  $1.9n^2$ ).

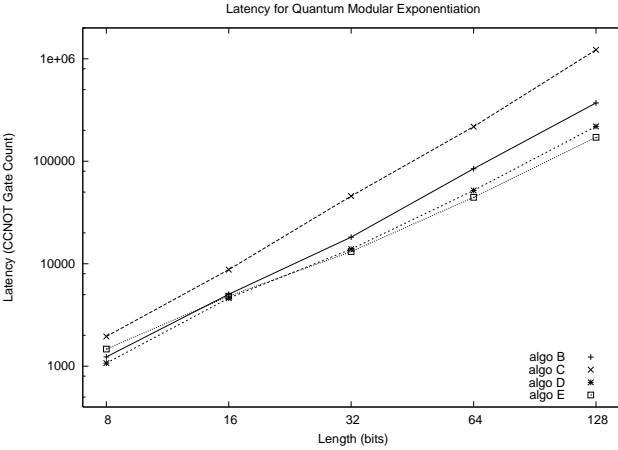


FIG. 16: Execution time for our algorithms for space  $100n$  on the  $AC$  architecture, for varying value of  $n$ .

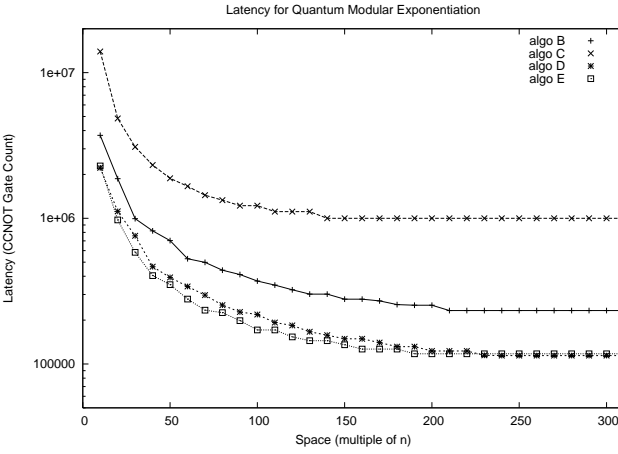


FIG. 17: Execution time for our algorithms for 128 bits on the  $AC$  architecture, for varying multiples of  $n$  space available.

### I. Asymptotic Behavior

The focus of this paper is the constant factors in modular exponentiation for important problem sizes and architectural characteristics. However, let us look briefly at the asymptotic behavior.

In section III D, we showed that our overall algorithm is

$$O(n/s + \log s) * \text{cost of multiplication} \quad (57)$$

Our multiplication algorithm is still

$$O(n) * \text{cost of addition} \quad (58)$$

Using carry-select adders, the cost of addition has improved to  $O(\sqrt{n})$  on  $AC$  and  $TC$ , though it remains  $O(n)$  on  $NTC$ ,

based on equations 15, 38, and 40. This gives total circuit depth of

$$BEXP_{AC} = BEXP_{TC} = O(n^{3/2}(n/s + \log s)) \quad (59)$$

$$BEXP_{NTC} = CEXP_{NTC} = O(n^2(n/s + \log s)) \quad (60)$$

As  $s \rightarrow n$ , these approach  $O(n^{3/2} \log n)$  and  $O(n^2 \log n)$ , respectively. Space requirements are  $O(ns)$  for all architectures.

Both **D** and **E** use an  $O(\log n)$  adder, giving

$$DEXP_{AC} = EEXP_{AC} = O((n \log n)(n/s + \log s)) \quad (61)$$

As  $s \rightarrow n$ , these approach  $O(n \log^2 n)$  and space consumed approaches  $O(n^2)$ .

This compares to asymptotic behavior of  $O(n^3)$  for VBE, BCDP, and **A**, using  $O(n)$  space. The limit of performance, using a carry-save multiplier and large  $s$ , will be  $O(\log^3 n)$  in  $O(n^3)$  space.

### V. CONCLUSION AND FUTURE WORK

Not all physically realizable architectures map cleanly to one of our models. A full two-dimensional mesh, such as neutral atoms in an optical lattice [27], and a loose trellis topology [28] probably fall between  $TC$  and  $NTC$ . The behavior of the scalable ion trap [29] is not immediately clear. In this work, our contribution has focused on improved adders, concurrency, and overall algorithmic structure. It seems likely that further improvements can be found in the overall structure and by more closely examining the construction of multipliers from adders [22]. We also intend to pursue multipliers built from hybrid carry-save adders.

We have shown that it is possible to significantly accelerate modular exponentiation using a stable of techniques. We have provided exact gate counts, rather than asymptotic behavior, showing algorithms that are faster by a factor of 100 to 700, depending on architectural features, when  $100n$  qubits of storage are available. Neighbor-only ( $NTC$ ) machines can run algorithms such as addition in  $O(n)$  at best, when non-neighbor machines ( $AC$ ,  $TC$ ) can achieve  $O(\log n)$  performance.

### Acknowledgments

The authors would like to thank Eisuke Abe, Fumiko Yamaguchi, and Kevin Binkley of Keio University, Thaddeus Ladd of Stanford University, Seth Lloyd of MIT, and Y. Kawano and Y. Takahashi of NTT Basic Research Laboratories for helpful discussions.

- 
- [1] P. W. Shor, in *Proc. 35th Symposium on Foundations of Computer Science* (IEEE Computer Society Press, 1994), pp. 124–134.
- [2] V. Vedral, A. Barenco, and A. Ekert, Phys. Rev. A **54**, 147 (1996), <http://arXiv.org/quant-ph/9511018>.
- [3] D. Beckman, A. N. Chari, S. Devabhaktuni, and J. Preskill, Phys. Rev. A **54**, 1034 (1996), <http://arXiv.org/quant-ph/9602016>.
- [4] R. Cleve and J. Watrous, in *Proc. 41st Annual Symposium on Foundations of Computer Science* (ACM, 2000), pp. 526–536.
- [5] P. Gossett, *Quantum carry-save arithmetic*, <http://arXiv.org/quant-ph/9808061> (1998).
- [6] C. Zalka, *Fast versions of Shor's quantum factoring algorithm*, <http://arXiv.org/quant-ph/9806084> (1998), <http://arXiv.org/quant-ph/9806084>.
- [7] C. Moore and M. Nilsson, SIAM J. Computing **31**, 799 (2001), <http://arxiv.org/abs/quant-ph/9808027>.
- [8] D. Loss and D. P. DiVincenzo, Phys. Rev. A **57**, 120 (1998).
- [9] B. E. Kane, Nature **393**, 133 (1998).
- [10] T. D. Ladd, J. R. Goldman, F. Yamaguchi, Y. Yamamoto, E. Abe, and K. M. Itoh, Physical Review Letters **89** (2002).
- [11] Y. A. Pashkin, T. Yamamoto, O. Astafiev, Y. Nakamura, D. V. Averin, and J. S. Tsai, Nature **421**, 823 (2003).
- [12] J. Q. You, J. S. Tsai, and F. Nori, Phys. Rev. Lett. **89** (2002), <http://arXiv.org/cond-mat/0306209>.
- [13] A. Barenco, C. H. Bennett, R. Cleve, D. P. DiVincenzo, N. Margolus, P. Shor, T. Sleator, J. Smolin, and H. Weinfurter, Phys. Rev. A **52**, 3457 (1995).
- [14] L. M. K. Vandersypen, Ph.D. thesis, Stanford University (2001), <http://arXiv.org/quant-ph/0205193>.
- [15] A. V. Aho and K. M. Svore, *Compiling quantum circuits using the palindrome transform*, <http://arXiv.org/quant-ph/0311008> (2003).
- [16] Y. Kawano, S. Yamashita, and M. Kitagawa (2004), private communication, submitted to PRA.
- [17] N. Kunihiro (2004), private communication.
- [18] Y. Takahashi, Y. Kawano, and M. Kitagawa, in [30].
- [19] A. Yao, in *Proceedings of the 34th Annual Symposium on Foundations of Computer Science* (Institute of Electrical and Electronic Engineers Computer Society Press, Los Alamitos, CA, 1993), pp. 352–361, URL [citeseer.ist.psu.edu/yao93quantum.html](http://citeseer.ist.psu.edu/yao93quantum.html).
- [20] G. Ahokas, R. Cleve, and L. Hales, in [30].
- [21] R. Van Meter, in *Proc. Int. Symp. on Mesoscopic Superconductivity and Spintronics (MS+S2004)* (2004).
- [22] M. D. Ercegovac and T. Lang, *Digital Arithmetic* (Morgan Kaufmann, 2004).
- [23] T. G. Draper, S. A. Kutin, E. M. Rains, and K. M. Svore, *A logarithmic-depth quantum carry-lookahead adder*, <http://arXiv.org/quant-ph/0406142> (2004), <http://arXiv.org/quant-ph/0406142>.
- [24] S. Beauregard, Quantum Information and Computation **3**, 175 (2003), <http://arXiv.org/quant-ph/0205095>.
- [25] T. G. Draper, *Addition on a quantum computer*, <http://arXiv.org/quant-ph/0008033> (2000), <http://arXiv.org/quant-ph/0008033>; first draft dated Sept. 1998.
- [26] M. A. Nielsen and I. L. Chuang, *Quantum Computation and Quantum Information* (Cambridge University Press, 2000), pp. 266–268.
- [27] G. K. Brennen, C. M. Caves, P. S. Jessen, and I. H. Deutsch, Physical Review Letters **82**, 1060 (1999).
- [28] M. Oskin, F. T. Chong, I. L. Chuang, and J. Kubiatowicz, in *Computer Architecture News, Proc. 30th Annual International Symposium on Computer Architecture* (ACM, 2003).
- [29] D. Kielpinski, C. Monroe, and D. J. Wineland, Nature **417**, 709 (2002).
- [30] *Proc. ERATO Conference on Quantum Information Science (EQIS2003)* (2003).
- [31] Shor noted this in his original paper, without explicitly specifying a bound. Note also that this bound is for a Turing machine; a random-access machine can reach  $O(n \log n)$ .
- [32] Zalka says 8 kilobits, but our basic algorithm is faster than his.
- [33] When we write ADDER in all capital letters, we mean the complete VBE  $n$ -bit construction, with the necessary undo; when we write adder in small letters, we are usually referring to a smaller or generic circuit block.
- [34] All calculations for space and latency are done in Octave (<http://www.octave.org>). Scripts available from the author.
- [35] We can perform this propagation at the beginning of the multiplication, in exchange for room to keep extra copies of  $|a\rangle$  in a few places. We will put a copy of  $|a\rangle$  in each carry-select group.
- [36] The circuit is too large to display in a figure, but a version for the six-bit carry-select adder is available for inspection from the author.